Commun Nonlinear Sci Numer Simulat 19 (2014) 1600–1610

Contents lists available at ScienceDirect

Commun Nonlinear Sci Numer Simulat

journal homepage: www.elsevier.com/locate/cnsns

Analysis of a modified two-lane lattice model by considering the density difference effect

Arvind Kumar Gupta *, Poonam Redhu

Department of Mathematics, Indian Institute of Technology Ropar, Punjab 140001, India

ARTICLE INFO

Article history:
Received 2 January 2013
Received in revised form 8 August 2013
Accepted 22 September 2013
Available online 8 October 2013

Keywords:
Traffic flow
Lattice model
Burgers equation
mKdV equation
Simulation

ABSTRACT

In this paper, a modified lattice hydrodynamic model of traffic flow is proposed by considering the density difference between leading and following lattice for two-lane system. The effect of density difference on the stability of traffic flow is examined through linear stability analysis and shown that the density difference term can significantly enlarge the stability region on the phase diagram. To describe the phase transition of traffic flow, the Burgers equation and mKdV equation near the critical point are derived through nonlinear analysis. To verify the theoretical findings, numerical simulation is conducted which confirms that traffic jam can be suppressed efficiently by considering the density difference effect in the modified lattice model for two-lane traffic.

1. Introduction

Due to rapid increase of automobile on roads, an enormous number of attempts have been made in the past to develop traffic flow model which can efficiently handle traffic jam situations and can analyze the jamming transition evolution of traffic flow. Various types of modeling approaches such as car-following model, cellular automata model, gas kinetic model and hydrodynamic models [1–3] have been used and well studied in the last few decades. Recently, lattice hydrodynamic model firstly proposed by Nagatani [4], which is a simplified version of macroscopic model and also incorporates the ideas of car-following models has been given much attention. The basic idea behind such models is that drivers adjust their velocity according to the observed headway. Subsequently, many extensions [5,7–18] to the Nagatani's work have been carried out by considering different factors into account like backward effect [5], lateral effect of the lane width [6] and anticipation effect of potential lane changing [7]. Recently, Tian et al. [8] developed a more realistic lattice hydrodynamic model for single lane by considering the effect of density difference and concluded that this effect leads to stabilize the traffic flow. Most of the above cited models describe some traffic phenomena only on single lane.

Furthermore, the lattice models were applied to a two-lane highway [19] and also to high-dimensional traffic flow by Nagatani [20]. Peng [21] extended the lattice hydrodynamic model by considering the optimal current difference of two-lane highway.

However, above models did not study the effect of density difference on two-lane highway where lane changing is allowed from one lane to another. In this paper, a modified lattice hydrodynamic model is proposed by introducing the density difference between the leading and the following lattice for two-lane highway. The linear stability and the neutral

* Corresponding author. Tel.: +91 1881 242140; fax: +91 1881 223395.
E-mail address: akgupta@iitrpr.ac.in (A.K. Gupta).
URL: http://www.iitrpr.ac.in/mathematics/akgupta (A.K. Gupta).

1007-5704/$ - see front matter © 2013 Elsevier B.V. All rights reserved.
http://dx.doi.org/10.1016/j.cnsns.2013.09.027

stability conditions are obtained. The Burgers equation is derived to describe a train of triangular shock wave. The mKdV equation is also derived and the kink-antikink solution is obtained near the critical point.

The paper is organized as follows. In the following section, a more realistic lattice model for two-lane is presented. In Section 3, the linear stability analysis is studied for the proposed model. Section 4 is devoted to the nonlinear analysis in which Burgers equation and mKdV equation are derived. Numerical simulations are carried out in Section 5 and finally, conclusions are given in Section 6.

2. A modified model

A simplified version of continuum model to describe the traffic phenomena on a single lane, proposed by Nagatani [4] in 1998 is

$$\partial_t \rho + \rho_0 \partial_x(\rho v) = 0, \tag{1}$$

$$\partial_t(\rho v) = a[\rho_0 V(\rho(x+\delta)) - \rho v], \tag{2}$$

where ρ_0 is the average density, a is the sensitivity of drivers, $V(.)$ is the optimal velocity function, $\rho(x+\delta)$ represents the density at position $x+\delta$ at time t, v and $\delta = 1/\rho_0$ are the velocity and the average headway, respectively.

The above simplified hydrodynamic model is further modified with dimensionless space x (let $x = x^*/\delta$ and x^* indicated as x hereafter) and expressed as

$$\partial_t \rho_j + \rho_0(\rho_j v_j - \rho_{j-1} v_{j-1}) = 0, \tag{3}$$

$$\partial_t(\rho_j v_j) = a[\rho_0 V(\rho_{j+1}) - \rho_j v_j]. \tag{4}$$

Eqs. (3) and (4) represent the lattice version of system of Eqs. (1) and (2), where j indicates site j on the one-dimensional lattice, ρ_j and v_j, respectively, represent the local density and velocity on site j at time t.

Recently, based on Nagatani's model, Tian et al. [8] proposed a density difference lattice model (DDLM) for a single lane traffic flow given by

$$\partial_t \rho_j + \rho_0(\rho_j v_j - \rho_{j-1} v_{j-1}) = 0, \tag{5}$$

$$\partial_t(\rho_j v_j) = a[\rho_0 V(\rho_{j+1}) - \rho_j v_j] + \lambda \frac{(\rho_j - \rho_{j-1})}{\rho_0}, \tag{6}$$

where ρ_0 is the average density, ρ and v denotes the local density and velocity, respectively. j indicates the j^{th} site on the one-dimensional lattice, $V(.)$ is the optimal velocity function and λ is the reaction coefficient to the density difference. When $\lambda = 0$, then the model becomes exactly the same as Nagatani's model [4]. By introducing density difference term in the evolution equation, the stability region of DDLM in the phase diagram is found to be larger than that of Nagatani's model and in DDLM [8] case, the vehicles dynamics also become more realistic than Nagatani's model.

In the literature of traffic flow, multi-lane models are found to be more accurately describe the flow as most of the road networks are made up of two or more lanes. In this paper, an attempt has been made to extend DDLM for a two-lane highway as follows:

Let us consider a two-lane highway on which DDLM is applied if there is no lane change allowed. Fig. 1 shows the schematic model of traffic flow on a two-lane highway.

The lane change occurs only in the following possibilities:

1. If the density at site $j-1$ on the first lane is higher than that at site j on the second lane, the lane changing occurs from the first lane to the second lane and will be proportional to their density difference as follows: $\gamma|\rho_0^2 V'(\rho_0)|\left(\rho_{1j-1}(t) - \rho_{2j}(t)\right)$.

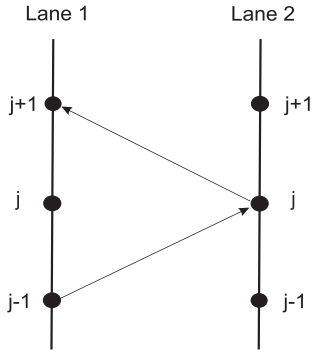

Fig. 1. The schematic diagram for traffic flow on two-lane highway.

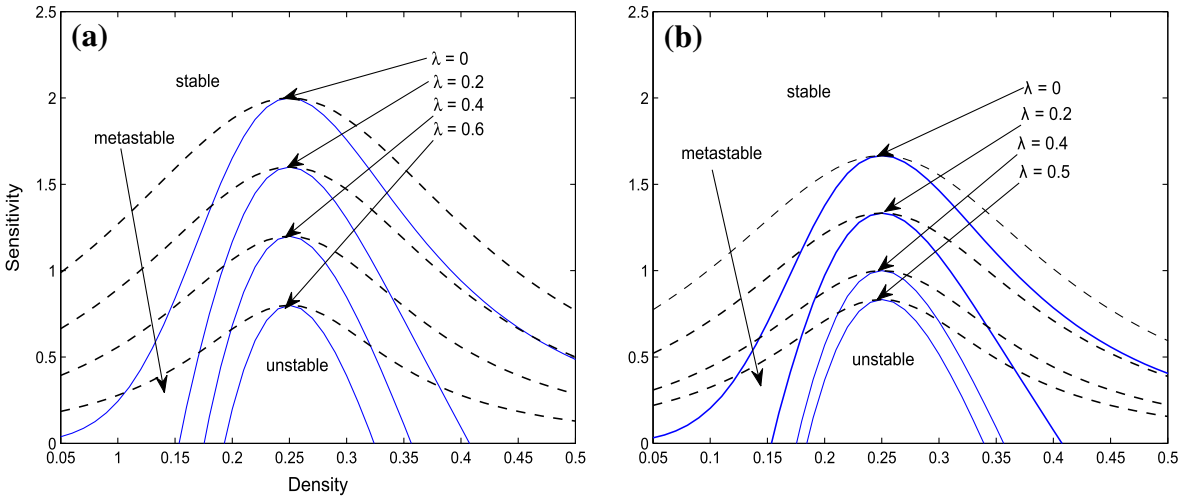

Fig. 2. Phase diagram in parameter space $(\rho; a)$, (a) $\gamma = 0$ and (b) $\gamma = 0.1$.

2. If the density at site j on the second lane is higher than that at site $j+1$ on the first lane, the lane changing occurs from the second lane to the first lane and will be proportional to their density difference as follows: $\gamma|\rho_0^2 V'(\rho_0)|\Big(\rho_{2j}(t) - \rho_{1j+1}(t)\Big)$.

Here, $\rho_{1j}(t)$ and $\rho_{2j}(t)$ are the densities on the first and second lane, respectively. The proportionality constant $(\gamma|\rho_0^2 V'(\rho_0)|)$ is chosen in such a way that it becomes dimensionless. Based on the above lane changing rules, the continuity equation for two-lane traffic can be obtained in the same fashion as of Nagatani [22] and is given by

$$\partial_t \rho_j + \rho_0(\rho_j v_j - \rho_{j-1} v_{j-1}) = \gamma|\rho_0^2 V'(\rho_0)|(\rho_{j+1} - 2\rho_j + \rho_{j-1}), \tag{7}$$

where $\rho_j = \frac{\rho_{1j}+\rho_{2j}}{2}$ and $\rho_j v_j = \frac{\rho_{1j}v_{1j}+\rho_{2j}v_{2j}}{2}$. Under the assumption that evolution equation of traffic current on each lane will not be affected by lane changing, the evolution equation for two-lane traffic [22] was incorporated as

$$\partial_t(\rho_j v_j) = a[\rho_0 V(\rho_{j+1}) - \rho_j v_j]. \tag{8}$$

Now, we present a more realistic evolution equation with the consideration of density difference as follows:

$$\partial_t(\rho_j v_j) = a[\rho_0 V(\rho_{j+1}) - \rho_j v_j] + \lambda\frac{(\rho_j - \rho_{j-1})}{\rho_0}. \tag{9}$$

From Eqs. (7) and (9), we obtain density equation by eliminating speed v as

$$\begin{aligned}&\partial_t^2\rho_j + a\rho_0^2\Big(V(\rho_{j+1}) - V(\rho_j)\Big) + a\partial_t\rho_j - a\gamma|\rho_0^2 V'(\rho_0)|(\rho_{j+1} - 2\rho_j + \rho_{j-1}) + \lambda(2\rho_j - \rho_{j+1} - \rho_{j-1})\\ &\quad - \gamma|\rho_0^2 V'(\rho_0)|(\partial_t\rho_{j+1} - 2\partial_t\rho_j + \partial_t\rho_{j-1})\\ &\quad = 0.\end{aligned} \tag{10}$$

It is clear from Eq. (10) that density at any site depends on forward as well as backward lattice. The theoretical and simulation results of DDLM model already shows that density difference between the leading and the following lattice stabilizes the traffic flow in a more realistic way on a single-lane [8].

3. Linear stability analysis

To investigate whether the proposed model can explain the jamming transition phenomena of traffic flow, we conducted linear stability analysis in this section. For this, the state of uniform traffic flow is taken as ρ_0 and optimal velocity $V(\rho_0)$, where ρ_0 is a constant. Hence, the steady-state solution of the homogeneous traffic flow is given by

$$\rho_j(t) = \rho_0, \quad v_j(t) = V(\rho_0). \tag{11}$$

Let $y_j(t)$ be a small perturbation to the steady-state density on site j. Then,

$$\rho_j(t) = \rho_0 + y_j(t). \tag{12}$$

Putting this perturbed density profile into Eq. (10) and linearizing it, we get

$$\partial_t^2 y_j(t) + a\rho_0^2 V'(\rho_0)\left[y_{j+1}(t) - y_j(t)\right] + \lambda\left[2y_j(t) - y_{j+1}(t) - y_{j-1}(t)\right] + a\partial_t y_j(t) - a\gamma|\rho_0^2 V'(\rho_0)|\left[y_{j+1}(t) - 2y_j(t) + y_{j-1}(t)\right] - \gamma|\rho_0^2 V'(\rho_0)|\left[\partial_t y_{j+1}(t) - 2\partial_t y_j(t) + \partial_t y_{j-1}(t)\right] = 0. \tag{13}$$

Substituting $y_j(t) = exp(ikj + zt)$ in Eq. (13), we obtain

$$z^2 + a\rho_0^2 V'(\rho_0)(e^{ik} - 1) + \lambda(2 - e^{ik} - e^{-ik}) + az + a\gamma|\rho_0^2 V'(\rho_0)|(e^{ik} - 2 + e^{-ik}) - \gamma|\rho_0^2 V'(\rho_0)|z(e^{ik} - 2 + e^{-ik}) = 0. \tag{14}$$

Inserting $z = ui$ in Eq. (14), with u being a real number and equating its real and imaginary parts, we have

$$-u^2 + a\rho_0^2 V'(\rho_0)(\cos k - 1) + \lambda(2 - 2\cos k) + a\gamma|\rho_0^2 V'(\rho_0)|(2\cos k - 2) = 0. \tag{15}$$

$$a\rho_0^2 V'(\rho_0)\sin k + au - \gamma|\rho_0^2 V'(\rho_0)|(2cosk - 2)u = 0. \tag{16}$$

From Eq. (16), we get

$$u = \frac{a\rho_0^2 V'(\rho_0)\sin k}{\gamma|\rho_0^2 V'(\rho_0)|(2cosk - 2) - a}. \tag{17}$$

Putting Eq. (17) into Eq. (15) and taking $k \to 0$, the neutral stability condition is obtained.

$$a = \frac{2\lambda - 2(\rho_0^2 V'(\rho_0))^2}{\rho_0^2 V'(\rho_0) + 2\gamma|\rho_0^2 V'(\rho_0)|}. \tag{18}$$

The traffic flow is stable for homogeneous condition if

$$a > \frac{2\lambda - 2(\rho_0^2 V'(\rho_0))^2}{\rho_0^2 V'(\rho_0) + 2\gamma|\rho_0^2 V'(\rho_0)|}. \tag{19}$$

For $\gamma = 0$, the above stability condition will reduce into

$$a > -2\rho_0^2 V'(\rho_0) + \frac{2\lambda}{\rho_0^2 V'(\rho_0)}, \tag{20}$$

which is exactly the same as for DDLM [8] and when $\lambda = 0$, we get the stability condition of Nagatani's model [17] as

$$a > -2\rho_0^2 V'(\rho_0). \tag{21}$$

Eq. (19) clearly shows that γ and reaction coefficient λ play an important role to stabilize the traffic flow. Solid curves in Fig. 2(a) and (b) shows the neutral stability curves in the phase space for $\gamma = 0$ and $\gamma = 0.1$ with respect to different values of λ. It can be easily depicted from the figures that the amplitude of these curves decreases with an increase in λ which means that larger value of λ leads to enlargement of stability region and hence, the traffic jam is suppressed efficiently. On comparing Fig. 2(a) and (b), it can be concluded that increase in the value of γ results a further increase in stable region which means that lane changing also reduces traffic jams significantly. This phenomenon is much closer to the real traffic as under the congested flow, vehicles try to accommodate themselves in a less denser lane by changing their lane quite frequently to overcome the jam situation.

4. Nonlinear stability analysis

4.1. Burgers equation and its solution

Using reduction perturbation method, we investigate the evolution characteristic of traffic jam around the critical point (ρ_c, a_c) on coarse-grained scales. Long-wavelength expansion method is used to understand the slowly varying behavior near the critical point. The slow variables X and T for a small positive scaling parameter $\epsilon(0 < \epsilon \ll 1)$ are defined as

$$X = \epsilon(j + bt), \quad T = \epsilon^2 t, \tag{22}$$

where b is a constant to be determined. Let ρ_j satisfy the following equation:

$$\rho_j(t) = \rho_c + \epsilon R(X, T). \tag{23}$$

Substituting Eqs. 22 and 23 into Eq. (10) and expanding the resulting equation to the third order of ϵ (see appendix A), we come across the following partial differential equation:

$$\epsilon^2\left[b + (\rho_c^2 V'(\rho_c))\partial_X R\right] + \epsilon^3\left[\partial_T R + \rho_c^2 V''(\rho_c)\partial_X R + \left(\frac{b^2 + \frac{a\rho_c^2 V'(p_c)}{2} - a\gamma|\rho_c^2 V'(\rho_c)| - \lambda}{a}\right)\partial_X^2 R\right] = 0. \tag{24}$$

By fixing $b = -\rho_c^2 V'(\rho_c)$, the second-order term of ϵ is eliminated from Eq. (24). Thus, we have

$$\partial_T R + \rho_c^2 V''(\rho_c)\partial_X R = -\left(\frac{\rho_c^4 V'(\rho_c)^2 + \frac{a\rho_c^2 V'(\rho_c)}{2} - a\gamma|\rho_c^2 V'(\rho_c)| - \lambda}{a}\right)\partial_X^2 R. \tag{25}$$

Since, the coefficient of the second derivative on the right hand side is positive in the linear stability region (Eq. 19). Eq. (25) is a Burgers equation in the stable freely moving traffic flow. The asymptotic solution for $T \gg 1$ is a train of N-triangular shock wave [23] and given as below:

$$R(X,T) = \frac{1}{|\rho_c^2 V''(\rho_c)|T}\left[X - \frac{1}{2}(\eta_n + \eta_{n+1})\right] - \frac{1}{2|\rho_c^2 V''(\rho_c)|T}(\eta_{n+1} - \eta_n) \times tanh\left[\frac{D}{4|\rho_c^2 V''(\rho_c)|T}(\eta_{n+1} - \eta_n)(X - \xi_n)\right], \tag{26}$$

where $D = -\left(\frac{\rho_c^4 V'(\rho_c)^2 + \frac{a\rho_c^2 V'(\rho_c)}{2} - a\gamma|\rho_c^2 V'(\rho_c)| - \lambda}{a}\right)$, the coordinates of shock fronts are given by $\xi_n, (n = 1, 2, 3, \ldots N)$ and η_n denotes the coordinates of the intersection of slope with the x-axis. As $T \to \infty, R(X,T) \to 0$, which means that any density wave expressed by Eq. (26) in the stable traffic flow region evolves into a uniform flow in due course of time and are shown in the Figs. 2(g) and 3(f).

4.2. mKdV Equation and its solution

Using the same reduction perturbation method as in previous subsection, we now obtain the mKdV equation to describe the traffic jam around the critical point (ρ_c, a_c). The slow variables X and T for $0 < \epsilon \ll 1$ are defined as below:

$$X = \epsilon(j + bt), \quad T = \epsilon^3 t, \tag{27}$$

where b is a constant to be determined. Let

$$\rho_j(t) = \rho_c + \epsilon R(X,T). \tag{28}$$

By expanding Eq. (10) to fifth order (see appendix A) of ϵ with the help of Eqs. (27) and (28), we obtain the following nonlinear equation:

$$\begin{aligned}
&\epsilon^2\left[a\rho_c^2 V'(\rho_c) + ab\right]\partial_X R + \epsilon^3\left[b^2 + \frac{a\rho_c^2 V'(\rho_c)}{2} - a\gamma|\rho_c^2 V'(\rho_c)| - \lambda\right]\partial_X^2 R + \\
&\epsilon^4\left[\left(\frac{a\rho_c^2 V'(\rho_c)}{6} - \gamma|\rho_c^2 V'(\rho_c)|b\right)\partial_X^3 R + \frac{a\rho_c^2 V\prime\prime\prime(\rho_c)}{6}\partial_X R^3 + a\partial_T R\right] + \\
&\epsilon^5\left[2b\partial_T\partial_X R + \left(\frac{a\rho^2 V'(\rho_c)}{24} - \frac{\lambda}{12} - \frac{a\gamma|\rho_c^2 V'(\rho_c)|}{12}\right)\partial_X^4 R + \frac{V\prime\prime\prime(\rho_c)}{12}a\rho_c^2\partial_X^2 R^3\right] = 0.
\end{aligned} \tag{29}$$

We set the deviation of sensitivity a from the critical point value a_c as

$$a_c = a(\epsilon^2 + 1), \quad b = -\rho_c^2 V'(\rho_c). \tag{30}$$

Using Eq. (30) and eliminating second and third order term of ϵ in Eq. (29), we get

$$\epsilon^4\left(\partial_T R - g_1\partial_X^3 R + g_2\partial_X R^3\right) + \epsilon^5\left(g_3\partial_X^2 R + g_4\partial_X^4 R + g_5\partial_X^2 R^3\right) = 0, \tag{31}$$

where, the coefficients g_i are given in the Table 1.

To convert Eq. (31) into a standard mKdV equation, the following transformations are used: $T' = g_1 T, R = \sqrt{\frac{g_1}{g_2}}R'$. Hence, Eq. (31) becomes

$$\partial_T R' - \partial_X^3 R' + \partial_X R'^3 + \epsilon M[R'] = 0, \tag{32}$$

where $M[R'] = \frac{1}{g_1}\left(g_3\partial_X^2 R' + \frac{g_1 g_5}{g_2}\partial_X^2 R'^3 + g_4\partial_X^4 R'\right)$. After ignoring the correction term in Eq. (32), we get the mKdV equation with kink-antikink solution as follows:

$$R_0'(X,T') = \sqrt{c}\tanh\left[\sqrt{\frac{c}{2}}(X - cT')\right]. \tag{33}$$

In order to determine the value of propagation velocity for the kink-antikink solution, it is necessary to satisfy the following condition:

$$(R_0', M[R_0']) \equiv \int_{-\infty}^{\infty} dX R_0' M[R_0'] = 0, \tag{34}$$

with $M[R_0'] = M[R']$. By solving Eq. (34), the selected value of c is

$$c = \frac{5g_2 g_3}{2g_2 g_4 - 3g_1 g_5}. \tag{35}$$

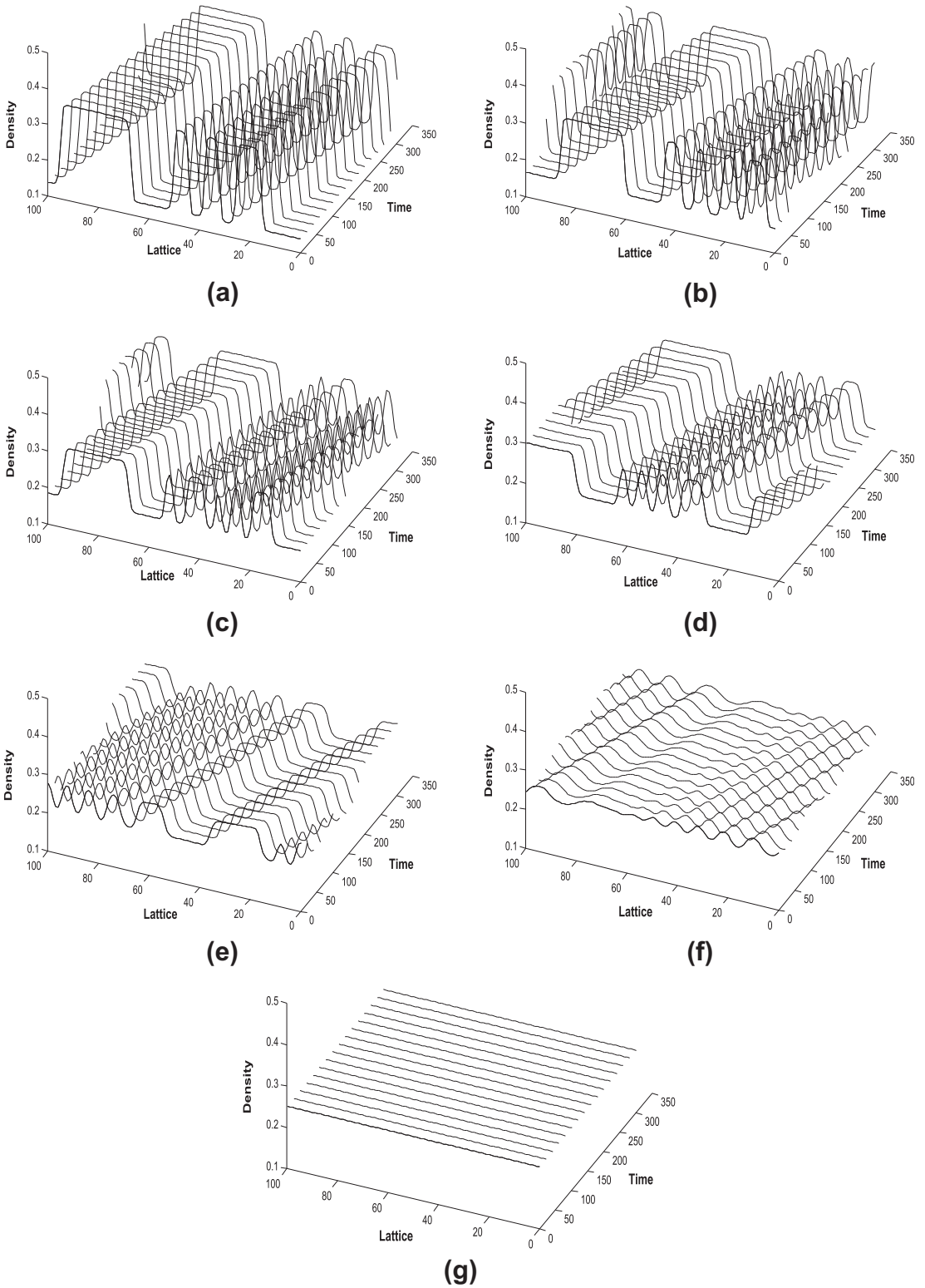

Fig. 3. Spatiotemporal evolutions of density when $\gamma = 0$ for (a) $\lambda = 0$, (b) $\lambda = 0.1$, (c) $\lambda = 0.2$,(d) $\lambda = 0.3$, (e) $\lambda = 0.4$, (f) $\lambda = 0.5$ and (g) $\lambda = 0.6$, respectively.

Table 1
The coefficients g_i of the model.

g_1	g_2	g_3
$-\rho_c^2 V'(\rho_c)\left(\frac{1}{6}+\frac{\gamma\lvert\rho_c^2 V'(\rho_c)\rvert}{a_c}\right)$	$\frac{V'''(\rho_c)\rho_c^2}{6}$	$\gamma\lvert\rho_c^2 V'(\rho_c)\rvert-\frac{\rho_c^2 V'(\rho_c)}{2}$
g_4		g_5
$\frac{\rho_c^2 V'(\rho_c)}{24}-\frac{\gamma\lvert\rho_c^2 V'(\rho_c)\rvert}{12}-\frac{\lambda}{12a_c}+\frac{\rho_c^4 V'(\rho_c)^2}{3a_c}+\frac{2\rho_c^4 V'(\rho_c)^2}{a_c^2}$		$\frac{\rho_c^2 V'''(\rho_c)}{12}+\frac{\rho_c^4 V'(\rho_c)V'''(\rho_c)}{3a_c}$

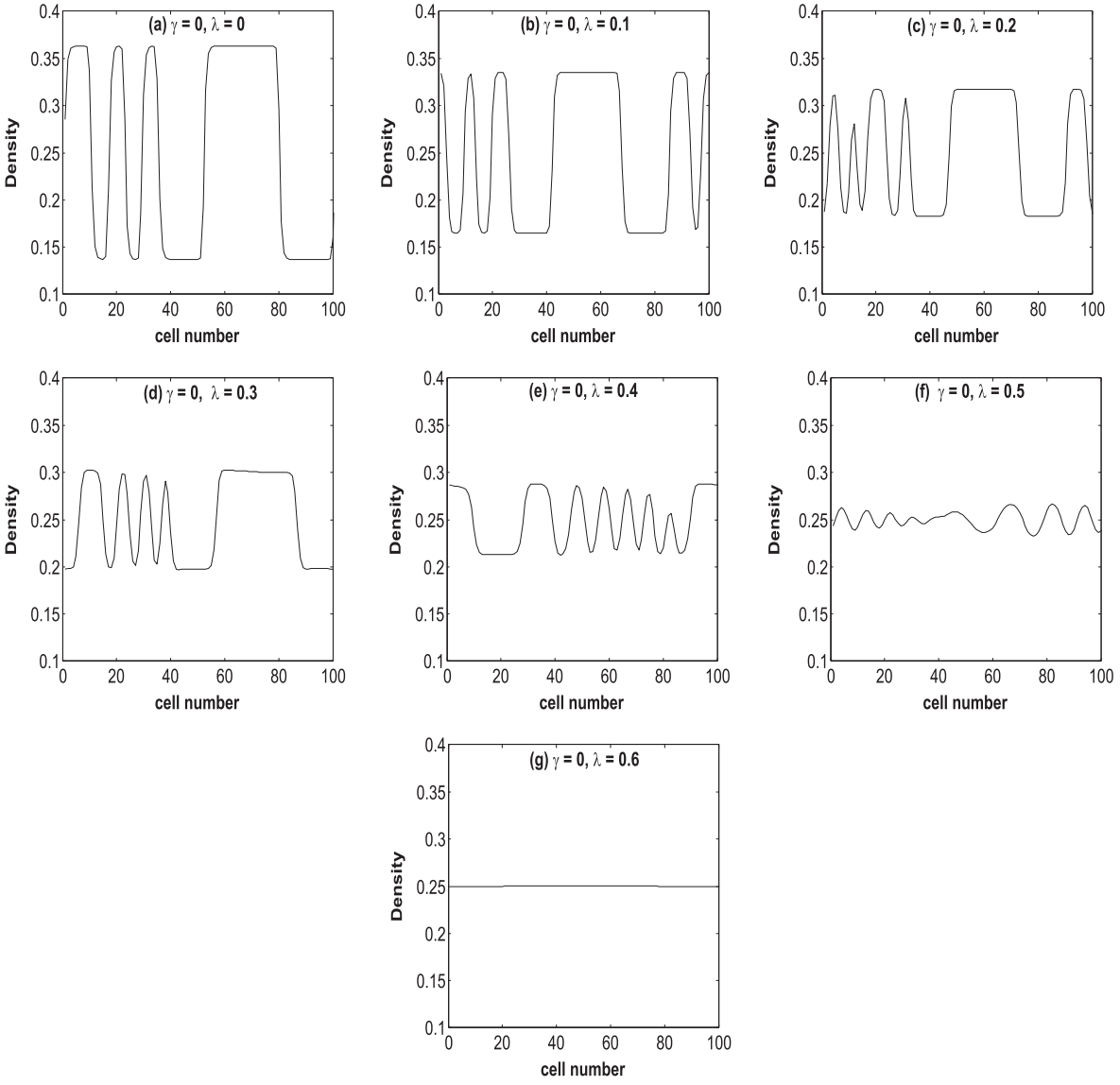

Fig. 4. Density profile at $t = 10300$ corresponding to Fig. 3, respectively.

Hence, the kink-antikink solution is given by

$$\rho_j = \rho_c + \epsilon\sqrt{\frac{g_1 c}{g_2}}\tanh\left(\sqrt{\frac{c}{2}}(X - cg_1 T)\right), \tag{36}$$

with $\epsilon^2 = \frac{a_c}{a} - 1$ and the amplitude A of the solution is

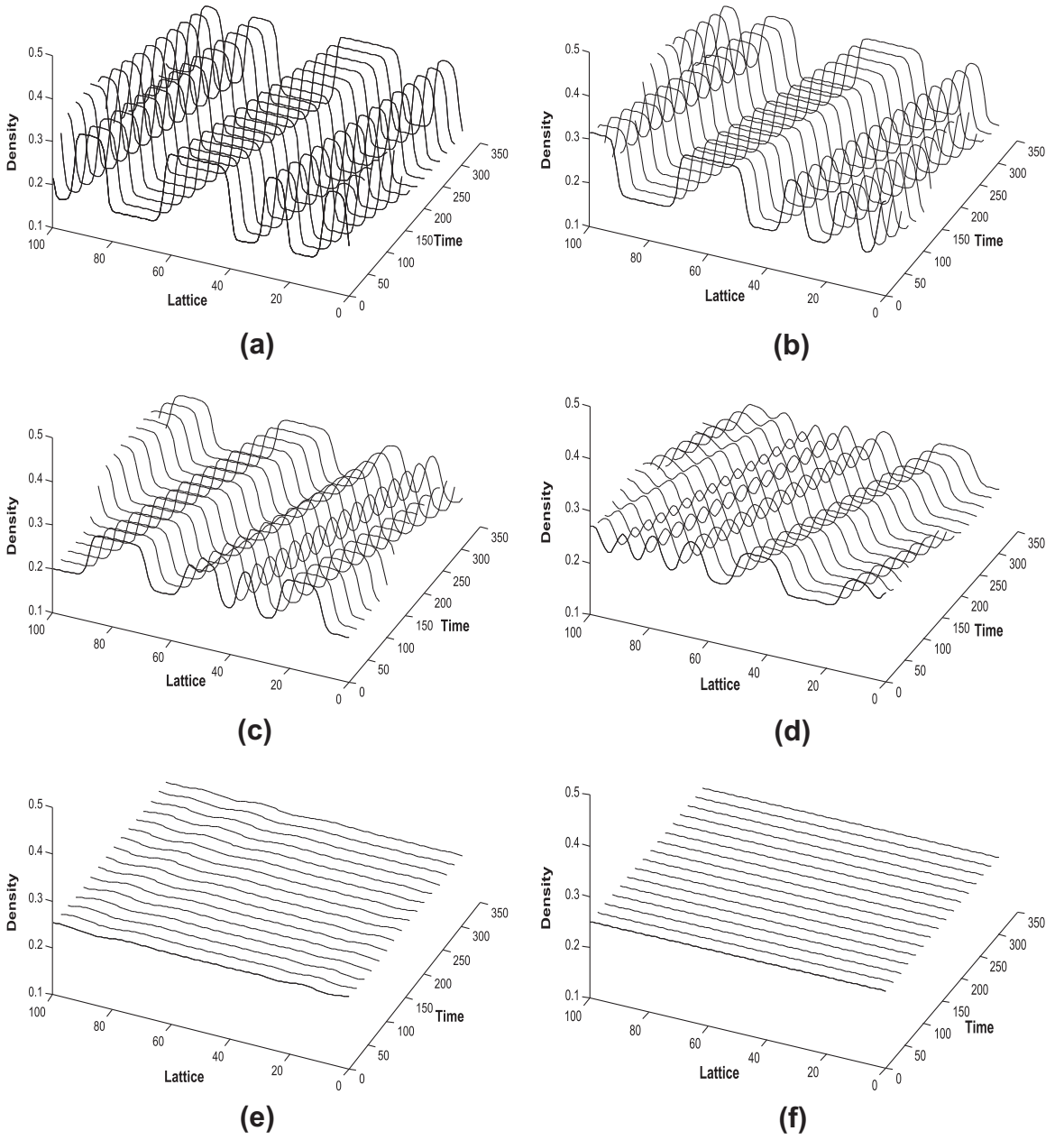

Fig. 5. Spatiotemporal evolutions of density when $\gamma = 0.1$ for (a) $\lambda = 0$, (b) $\lambda = 0.1$, (c) $\lambda = 0.2$, (d) $\lambda = 0.3$, (e) $\lambda = 0.4$ and (f) $\lambda = 0.5$, respectively.

$$A = \sqrt{\frac{g_1}{g_2}\epsilon^2 c}. \tag{37}$$

The kink-antikink solution represents the coexisting phase including both freely moving phase and congested phase which can be described by $\rho_j = \rho_c \pm A$, respectively in the phase space (ρ, a). For a particular case when $\gamma = 0$, the results become similar to those found by Tian [8] and for $\gamma = \lambda = 0$, the results are same as those obtained by Nagatani [17]. The dashed and solid lines in Fig. 2, respectively, represent the coexisting and neutral stability curves which divide the phase plane into three regions: stable, metastable and unstable. In the stable region above the coexisting curves, the traffic flow will remain stable under a disturbance in a nearly uniform traffic flow and traffic jams do not occur in this region while in unstable region, a small disturbance in a nearly uniform traffic flow will lead to the congested traffic and traffic jam appears. In the metastable region, when small disturbances are intervened into nearly uniform traffic, the traffic flow remains stable, however, when large amplitude disturbance occur, the traffic flow becomes unstable and moving jams emerge. In addition, with an increase

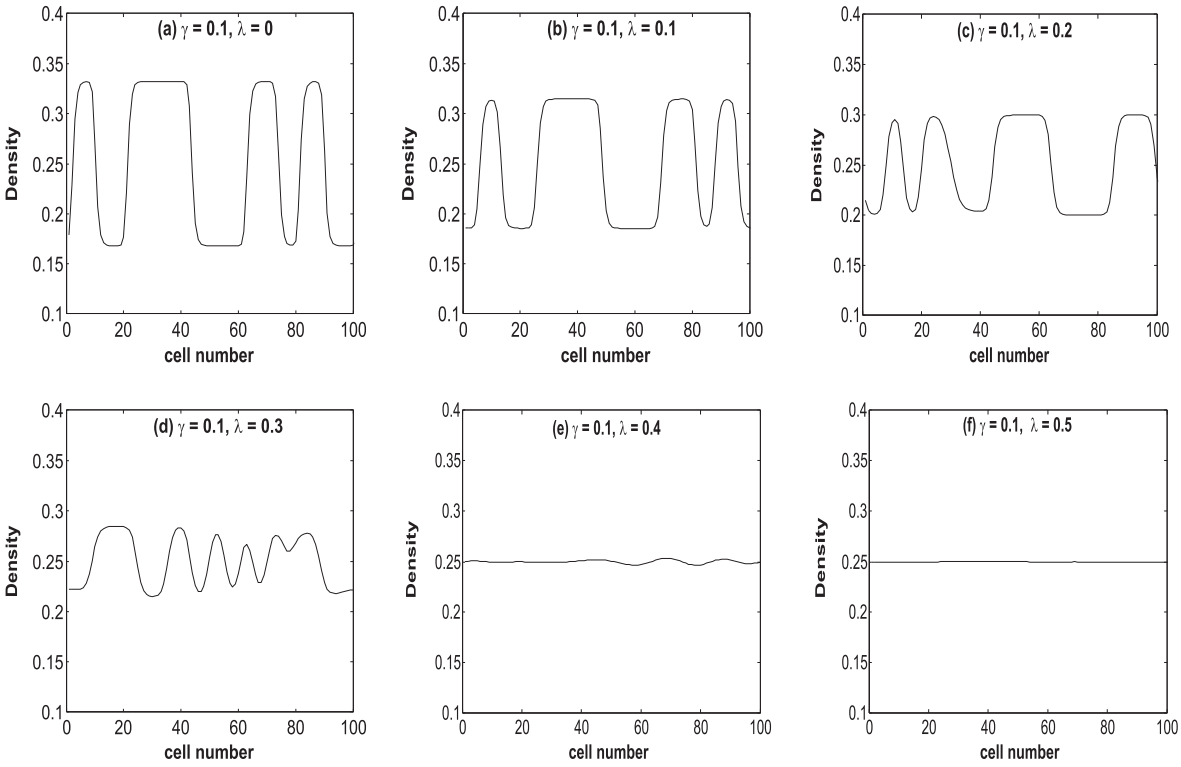

Fig. 6. Density profile at $t = 10300$ corresponding to Fig. 5, respectively.

of γ and reaction coefficient λ, the corresponding neutral and coexisting curves both lower down, which means that the effect of both the parameters can further stabilize the traffic flow.

5. Numerical Simulation

For numerical computation, we rewrite the Eq. (10) in full difference form:

$$\begin{aligned}\rho_j(t+2\tau) = {} & 2\rho_j(t+\tau) - \rho_j(t) - a\tau^2\rho_0^2\Big[V(\rho_{j+1}) - V(\rho_j)\Big] - \lambda\tau^2[2\rho_j(t) - \rho_{j+1}(t) - \rho_{j-1}(t)] - a\tau\Big[\rho_j(t+\tau) - \rho_j(t)\Big] \\ & + a\tau^2\gamma|\rho_0^2V'(\rho_0)|\Big[\rho_{j+1}(t) - 2\rho_j(t) + \rho_{j-1}(t)\Big] \\ & + \tau\gamma|\rho_0^2V'(\rho_0)|\Big[(\rho_{j+1}(t+\tau) - 2\rho_j(t+\tau) + \rho_{j-1}(t+\tau)) - (\rho_{j+1}(t) - 2\rho_j(t) + \rho_{j-1}(t))\Big]. \end{aligned} \tag{38}$$

To validate the theoretical findings, the numerical simulation is carried out for the extended model described by Eq. (38). Periodic boundary conditions are adopted and the initial density profile is set as follows:

$$\rho_j(1) = \rho_j(0) = \begin{cases} \rho_0; & j \neq \frac{M}{2}, \quad \frac{M}{2}+1 \\ \rho_0 - \sigma; & j = \frac{M}{2} \\ \rho_0 + \sigma; & j = \frac{M}{2}+1 \end{cases}, \tag{39}$$

where σ is the initial disturbance, the total number of sites M is taken as 100 and other parameters are set as follows: $\sigma = 0.05, a = 1, \tau = 0.1$.

The optimal velocity function given by Nagatani [22] is adopted.

$$V(\rho) = \frac{v_{max}}{2}\left[\tanh\left(\frac{2}{\rho_0} - \frac{\rho}{\rho_0^2} - \frac{1}{\rho_c}\right) + \tanh\left(\frac{1}{\rho_c}\right)\right], \tag{40}$$

where v_{max} and ρ_c denotes the maximal velocity and the safety critical density. The optimal velocity function is monotonically decreasing, has an upper bound and a turning point at $\rho = \rho_c = \rho_0$. For computation, maximal velocity and critical density are set at 2 and 0.25, respectively.

Fig. 3 shows the simulation results after 10^4 time steps for different values of λ when lane changing is not permitted ($\gamma = 0$). It is clear from the Fig. 3(a)–(f) that the initial dist urbance leads to the kink-antikink soliton which propagates in the backward direction. Due to this, initial disturbance evolves into congested flow as the stability condition is not satisfied. Fig. 3(g) depicts that as soon as $\lambda = 0.6$ i.e. we enter into stable region, the small amplitude perturbation to the homogeneous density dies out. Furthermore, Eq. (26) also demonstrates that in the stable region any disturbance will evolve into a uniform flow in due course of time. Therefore, from the theoretical analysis as well as simulation results, one can conclude that the traffic jam can be suppressed effectively by taking the density difference effect of two-lane into account.

Fig. 4 describes the density profile at sufficiently large time $t = 10300$ corresponding to Fig. 3. It is also clear from Fig. 4 that for small values of λ, a nonlinear wave with kink-antikink form similar to the solution of mKdV equation appears and propagates backward. This situation exhibits the stop and go waves in traffic flow. The amplitude of the density wave decreases and converts into an oscillatory traffic and finally, evolves into uniform flow with an increase in λ. In this regard, our model is more realistic in comparison to Peng's model ([21]), the dipole like structure firstly converts into small amplitude stop and go wave, which dies out as reaction coefficient increases.

Figs. 5 and 6 show the simulation results under the different values of λ when lane changing is permitted ($\gamma = 0.1$). The results corresponding to $\gamma = 0.1$ are qualitatively similar to those obtained for $\gamma = 0$. Parallel to no lane changing situation, initially kink-antkink soliton occurs and propagates in the backward direction. Since, the stability condition is not satisfied, the initial small perturbation on the uniform flow evolves into congested flow. However, density waves disappears and the traffic flow becomes stable under the larger effect of reaction coefficient. It is clear from the density profile that the traffic flow becomes stable for quite small value of reaction coefficient for lane changing in comparison to without lane changing situation. As a result, it is reasonable to infer that the reaction coefficient as well as lane changing effect improve the stability of traffic flow. Based on the analytical and simulation results, we can conclude that traffic jam can be suppressed more effectively by considering density difference effect for two-lane system.

6. Conclusion

A modified lattice hydrodynamic traffic flow model for two-lane highway has been proposed by considering the density difference effect between the leading and following lattice to describe the jamming transition. By using reductive perturbation method, the stability criterion is obtained through linear stability analysis. Furthermore, nonlinear stability analysis has carried out to obtain Burgers and mKdV equation near the critical point. Phase diagrams in the density-sensitivity space with the neutral stability curves and the coexisting curves are given for different values of γ and reaction coefficient λ. It can be seen that with the increase the value of γ or λ, the unstable region reduces. Numerical simulation shows that drivers behavior in terms of lane changing become more realistic when approaching jams. It is also shown that density difference effect plays an important role in stabilizing the traffic flow on two-lane highway. The simulation results are in accordance with the theoretical findings.

Acknowledgement

The second author acknowledges Council of Scientific and Industrial Research, India for providing financial assistance.

Appendix A

In this appendix, we give the expansion of each term in Eq. (10) using Eq. (27) and Eq. (28) to the fifth-order of ϵ.

$$\partial_t \rho_j = \epsilon^2 b \partial_X R + \epsilon^4 \partial_T R, \tag{A.1}$$

$$\partial_t^2 \rho_j = \epsilon^3 b \partial_X^2 R + 2b\epsilon^5 \partial_X \partial_T R, \tag{A.2}$$

$$\rho_{j+1} = \rho_c + \epsilon R + \epsilon^2 \partial_X R + \frac{\epsilon^3}{2}\partial_X^2 R + \frac{\epsilon^4}{6}\partial_X^3 R + \frac{\epsilon^5}{24}\partial_X^4 R, \tag{A.3}$$

$$\rho_{j-1} = \rho_c + \epsilon R - \epsilon^2 \partial_X R + \frac{\epsilon^3}{2}\partial_X^2 R - \frac{\epsilon^4}{6}\partial_X^3 R + \frac{\epsilon^5}{24}\partial_X^4 R, \tag{A.4}$$

$$\rho_{j+1} - 2\rho_j + \rho_{j-1} = \epsilon^3 \partial_X^2 R + \frac{\epsilon^5}{12}\partial_X^4 R. \tag{A.5}$$

The expansion of optimal velocity function at the turning point is

$$V(\rho_j) = V(\rho_c) + V'(\rho_c)(\rho_j - \rho_c) + \frac{V'''(\rho_c)}{6}(\rho_j - \rho_c)^3, \tag{A.6}$$

$$V(\rho_{j+1}) = V(\rho_c) + V'(\rho_c)(\rho_{j+1} - \rho_c) + \frac{V'''(\rho_c)}{6}(\rho_{j+1} - \rho_c)^3. \tag{A.7}$$

Using Eqs. A.6 and A.7, we get

$$V(\rho_{j+1}) - V(\rho_j) = V'(\rho_c)[\epsilon^2\partial_X R + \frac{\epsilon^3}{2}\partial_X^2 R + \frac{\epsilon^4}{6}\partial_X^3 R + \frac{\epsilon^5}{24}\partial_X^4 R] + \frac{V'''(\rho_c)}{6}[\epsilon^4\partial_X R^3 + \frac{\epsilon^5}{2}\partial_X^2 R^3]. \tag{A.8}$$

By inserting A.1, A.2, A.5 and A.8 into Eq. (10), we obtain Eq. (29).

References

[1] Jiang R, Wu Q, Zhu Z. A new continuum model for traffic flow and numercial test. Trans Res B 2002;36:405–19.
[2] Gupta AK, Katiyar VK. Analyses of shock wave and traffic jam. J Phys A: Math Gen 2005;38:4069–83.
[3] Tang TQ, Huang HJ, Shang HY. A new macro model for traffic flow with the consideration of the drivrs forecast effect. Phys Lett A 2010;374:1668–72.
[4] Nagatani T. Modified KdV equation for jamming transtion in the continuum models of traffic. Physica A 1998;261:599–607.
[5] Ge HX, Cheng RJ. The backward looking effect in the lattice hydrodynamic model. Physica A 2008;387:6952–8.
[6] Peng GH, Cai XH, Cao BF, Liu CQ. Non-lane-based lattice hydrodynamic model of traffic flow considering the lateral effects of the lane width. Phys Lett A 2011;375:2823–7.
[7] Peng GH, Cai XH, Liu CQ, Tuo MX. A new lattice model of traffic flow with the anticipation effect of potential lane changing. Phys Lett A 2012;376:447–51.
[8] Tian JF, Yuan ZZ, Jia B, Li MH, Jiang GJ. The stabilization effect of the density difference in the modified lattice hydrodynamic model of traffic flow. Physica A 2012;391:4476–82.
[9] Ge HX, Dai SQ, Xue Y, Dong LY. Stabilization analysis and modified Kortewegde Vries equation in a cooperative driving system. Phys Rev E 2005;71:066119.
[10] Ge HX. The Kortewegde Vries soliton in the lattice hydrodynamic model. Physica A 2009;388:1682–6.
[11] Ge HX, Cheng RJ, Lei L. The theoretical analysis of the lattice hydrodynamic models for traffic flow theory. Physica A 2010;389:2825–34.
[12] Li XL, Li ZP, Han XL, Dai SQ. Effect of the optimal velocity function on traffic phase transitions in lattice hydrodynamic models. Commun Nonlinear Sci Numer Simul 2009;14:2171–7.
[13] Li ZP, Li XL, Liu FQ. Stabilization analysis and modified KdV equation of lattice models with consideration of relative current. Int J Mod Phys C 2008;19:1163–73.
[14] Peng GH, Cai XH, Liu CQ, Cao BF. A new lattice model of traffic flow with the consideration of the drivers forecast effects. Phys Lett A 2011;375:2153–7.
[15] Peng GH, Cai XH, Cao BF, Liu CQ. A new lattice model of traffic flow with the consideration of the traffic interruption probability. Physica A 2012;391:656–63.
[16] Peng GH, Nie FY, Cao BF, Liu CQ. A drivers memory lattice model of traffic flow and its numerical simulation. Nonlinear Dyn 2012;67:1811–5.
[17] Nagatani T. TDGL and MKdV equations for jamming transition in the lattice models of traffic. Physica A 1999;264:581–92.
[18] Xue Y. Lattice model of the optimal traffic flow. Acta Phys Sin 2004;53:25–30.
[19] Nagatani T. Jamming transition in a two-dimensional traffic flow model. Phys Rev E 1999;59:4857–64.
[20] Nagatani T. Jamming transition of high-dimensional traffic dynamics. Physica A 1999;272:592–611.
[21] Peng GH. A new lattice model of two-lane traffic flow with the consideration of optimal current difference. Commun Nonlinear Sci Numer Simul 2013;18:559–66.
[22] Nagatani T. Jamming transition and the modified Korteweg-de Vaeies equation in a two-lane traffic flow. Physica A 1999;265:297–310.
[23] Tatsumi T, Kida S. Statistical mechanics of the Burger model of turbulence. Fluid Mech 1972;55:659.